How to cite: *Angew. Chem. Int. Ed.* **2023**, *62*, e202304150
doi.org/10.1002/anie.202304150

Fluorine Chemistry **Hot Paper**

Geometric Isomerisation of Bifunctional Alkenyl Fluoride Linchpins: Stereodivergence in Amide and Polyene Bioisostere Synthesis

Max Wienhold, Byeongseok Kweon, Calum McLaughlin, Matthias Schmitz, Till J. B. Zähringer, Constantin G. Daniliuc, Christoph Kerzig, and Ryan Gilmour**

Dedicated to Professor Erick M. Carreira on the occasion of his 60th birthday

Abstract: Amide groups are pervasive across the chemical space continuum, where their structural and pharmacological importance, juxtaposed with the hydrolytic vulnerabilities, continues to fuel bioisostere development. Alkenyl fluorides have a venerable history as effective mimics (Ψ[CF=CH]) owing to the planarity of the motif and intrinsic polarity of the C(sp^2)–F bond. However, emulating the *s-cis* to the *s-trans* isomerisation of a peptide bond with fluoro-alkene surrogates remains challenging, and current synthetic solutions only enable access to a single configuration. Through the design of an ambiphilic linchpin based on a fluorinated β-borylacrylate, it has been possible to leverage energy transfer catalysis to affect this unprecedented isomerisation process: this provides geometrically-programmable building blocks that can be functionalised at either terminus. Irradiation at $\lambda_{max} = 402$ nm with inexpensive thioxanthone as a photocatalyst enables rapid, effective isomerisation of tri- and tetra-substituted species (up to *E*/*Z* 98:2 in 1 h), providing a stereodivergent platform for small molecule amide and polyene isostere discovery. Application of the methodology in target synthesis and initial laser spectroscopic studies are disclosed together with crystallographic analyses of representative products.

Introduction

The evolutionary success of amides in the bioactive natural product repertoire has galvanised interest in emulating this venerable structural motif through bioisostere design.[1] In contemporary drug discovery, this strategy enables the pharmacological advantages of leveraging peptide bonds to be reconciled with their metabolic susceptibilities in vivo.[2] Whilst effective mimesis requires the electronic and structural footprint of the parent motif to be recreated, amides present an additional stereochemical challenge on account of *s-cis* to *s-trans* isomerisation.[3] This conspicuous feature of the amide bond is particularly relevant when biological function is encoded by configuration.[4] Alkenyl fluorides Ψ[CF=CH] have proven to be highly effective amide bond isosteres, where the polar nature of the C(sp^2)–F bond enables the steric and electronic signature of the native motif to be simulated (Figure 1A).[5] This ability to concurrently regulate configuration and protect enzymatically vulnerable sites[6] has been expertly leveraged to enhance the hydrolytic stability of HDAC inhibitors[7] and to increase plasma and microsomal stability in peptide mimetics such as Tyr^1-Ψ[(Z)CF=CH]–Gly^2 Leu-enkephalin (Figure 1B).[8] In the realm of kinase inhibitor design, installation of the *E*-fluoro-enone motif in 5-fluoroenoneresorcynolide has been advantageous in safeguarding the structural integrity of the API.[9]

A compelling example of the importance of alkenyl fluoride configuration on biological activity is illustrated by comparing the respective IC_{50} values of factor Xa inhibitors.[10] A seemingly subtle inversion of alkene geometry, from the *Z*- to *E*-isomer, results in a 60-fold enhancement, thereby demonstrating the value of sterodivergence platforms in enhancing bioactivity.

This strategic importance of mono-fluoro olefins in functional small molecule discovery continues to provide a powerful impetus for selective reaction development. Olefination strategies[11–14] have been key facilitators in enabling alkenyl fluorides to be validated as amide bond isosteres, but achieving satisfactory levels of stereocontrol continue to limit application. Whilst most methods favor formation of the (often lower-energy) *Z*-isomer,[15] strategies to enable the stereoselective preparation of the corresponding *E*-isomer are rare[16] and often suffer from scope limitations. These stoichiometric approaches have been complemented by advances in alkene cross metathesis[17–19] and selective defluoroborylation,[20] thereby allowing stereoselectivity to be regulated at the catalyst level. However, to the best of our knowledge, strategies to enable the simple *Z*→*E* isomer-

[*] M. Wienhold, B. Kweon, Dr. C. McLaughlin, Dr. C. G. Daniliuc, Prof. Dr. R. Gilmour
Organisch Chemisches Institut, Westfälische Wilhelms-Universität Münster
Corrensstraße 36, 48149 Münster (Germany)
E-mail: ryan.gilmour@uni-muenster.de
M. Schmitz, T. J. B. Zähringer, Prof. Dr. C. Kerzig
Department of Chemistry, Johannes Gutenberg University Mainz
Duesbergweg 10–14, 55128 Mainz (Germany)
E-mail: ckerzig@uni-mainz.de

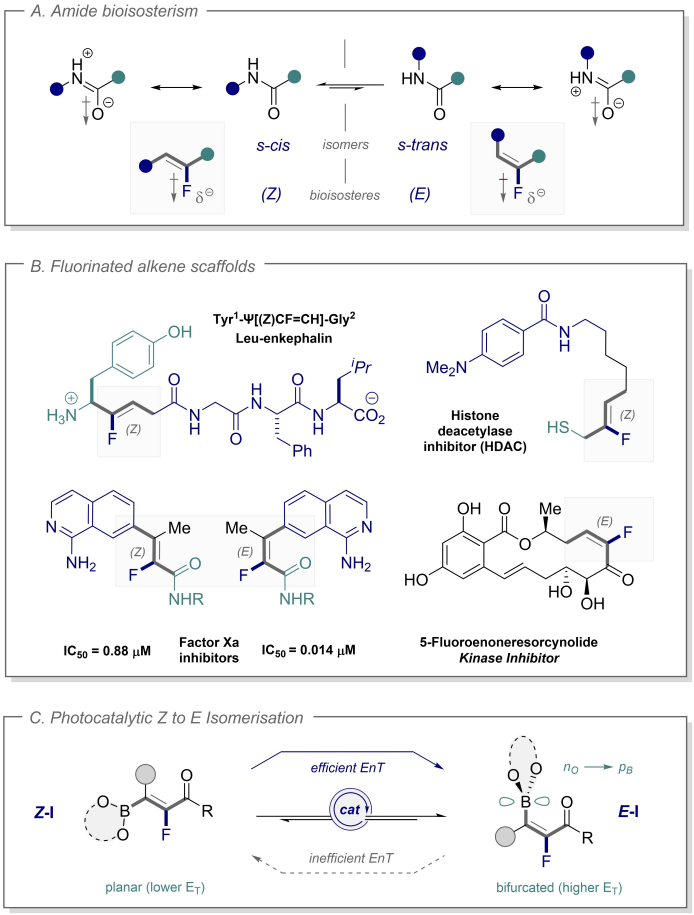

Figure 1. Alkenyl fluorides as amide bond bioisosteres and selected bioactive small molecules containing this structural motif.

isation of alkenyl fluorides are conspicuous in their absence (Figure 1C). Not only would this platform emulate the behavior of the native scaffold, but it would also mitigate the lengthy synthesis campaigns required to access both isomers independently.[5,21]

It was therefore envisaged that fluorinated β-boryl acrylates, such as ***Z*-I**, would be appealing starting materials from which to develop an operationally simple isomerisation protocol based on selective energy transfer catalysis.[22–24] Identification of an appropriate small molecule sensitizer would then allow selective excitation of the *Z*-isomer and accumulation of the desired *E*-configured product. In the starting *Z*-isomer, the planar chromophore includes the vacant *p*-orbital of the boron substituent, whereas Lewis-type $n_O \rightarrow p_B$ interactions bifurcates the chromophore in the product *E*-isomer. This results in 90° rotation of the C(sp^2)–B bond raises the triplet energy of the product and provides a foundation for directionality. In addition to their well-defined photophysical properties, these ambiphilic linchpins lend themselves to bidirectional, post-isomerisation functionalisation through stereospecific cross coupling and carbonyl modification chemistry. Furthermore, by extending the tri-substituted series to tetra-substitution,[25] analogs might be generated that would be suitable as both tertiary amides and as alkene surrogates for fluoro-mimetic development.[26]

Results and Discussion

Despite the efficiency of isomerisation in non-fluorinated systems,[22,23] we were acutely aware that fluorine incorporation would present a significant challenge in the working blueprint: structurally related aryl boronic esters and acids bearing halogen substituents in the *ortho*-position are susceptible to a range of decomposition pathways.[27] Consequently, the robust pinanediol boronic ester was selected for further exploration. To validate the working hypothesis, the conversion of ***Z*-1** to ***E*-1** was investigated using a range of simple organic photosensitizers with varying triplet energies (Table 1). Whilst initial attempts to affect isomerisation with 9-fluorenone ($\lambda = 402$ nm) proved to be unsuccessful (*E*:*Z* = 8:92, Table 1, entry 1), catalysts with higher triplet energies proved to be more effective. Isomerisation with Michler's ketone ($\lambda = 365$ nm) led to an enhanced selectivity (*E*:*Z* = 54:46, entry 2) albeit at the expense of the yield. Extending the trend further to catalysts with higher triplet energies, such as thioxanthone and benzophenone, enabled the desired product to be obtained with good

Table 1: Reaction optimisation of the energy transfer-enabled isomerisation.[a]

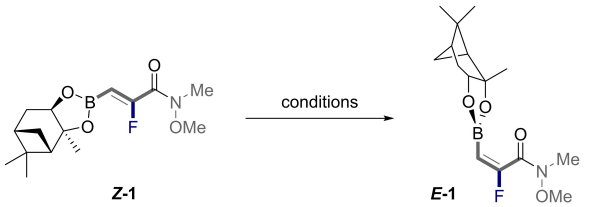

entry	catalyst	wavelength λ [nm]	E_T [kJ mol^{-1}]	yield [%][b]	E/Z[c]
1	9-fluorenone	402	223	98	8:92
2	Michler's Ketone	365	255	27	54:46
3	thioxanthone	402	265	87	91:9
4	benzophenone	365	289	90	94:6
5[d]	benzophenone	365	289	60	60:40
6[d]	thioxanthone	402	265	86 (53)	95:5
7[d]	thioxanthone	/	265	>98	<1:99
8[d]	/	402	/	>98	<1:99

[a] Reactions were conducted in MeCN under irradiation for 16 h. [b] Determined by ^{1}H NMR using 1,3,5-trimethoxybenzene as the internal standard; isolated yield reported in parenthesis. [c] Determrmined from the crude reaction mixture. [d] Reaction time 1 h.

yields and selectivities ($E:Z = 91:9$ and $= 94:6$, entries 3 and 4) after 16 h. Although reactions with benzophenone required extended reaction times (entry 4 versus 5), it was possible to reach high levels of selectivity after only 1 h with thioxanthone (entry 6, E/Z 95:5). Moreover, control reactions in the absence of light and photocatalysts support the postulated energy transfer paradigm (entries 7 and 8).

The presence of the fluorine atom allowed the conversion of ***Z*-1** (−93.64 ppm) to ***E*-1** (−84.52 ppm) to be conveniently monitored by time course ^{19}F NMR spectroscopy. As is evident from Figure 2, the isomerisation proceeds smoothly and the photostationary composition is reached after 60 minutes.

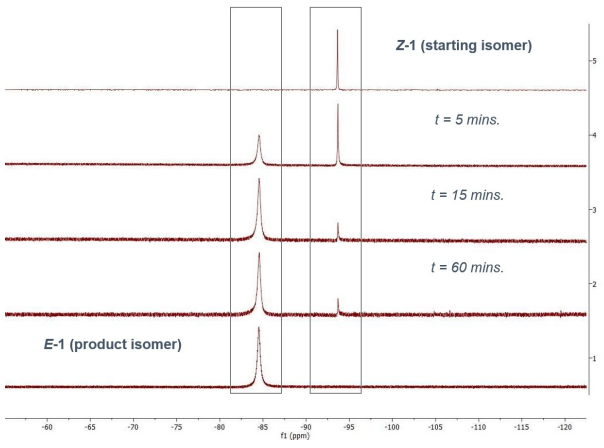

Figure 2. Time course study of the photochemical isomerisation. From top to bottom: [5] Starting material ***Z*-1**, [4] Reaction mixture after 5 min irradiation time, [3] Reaction mixture after 15 min irradiation time, [2] Reaction mixture after 60 min irradiation time, [1] Isolated product ***E*-1**.

To establish the scope and limitations of the photocatalytic isomerisation of alkenyl fluorides, the impact of modifying the carbonyl substituent was explored (Figure 3).

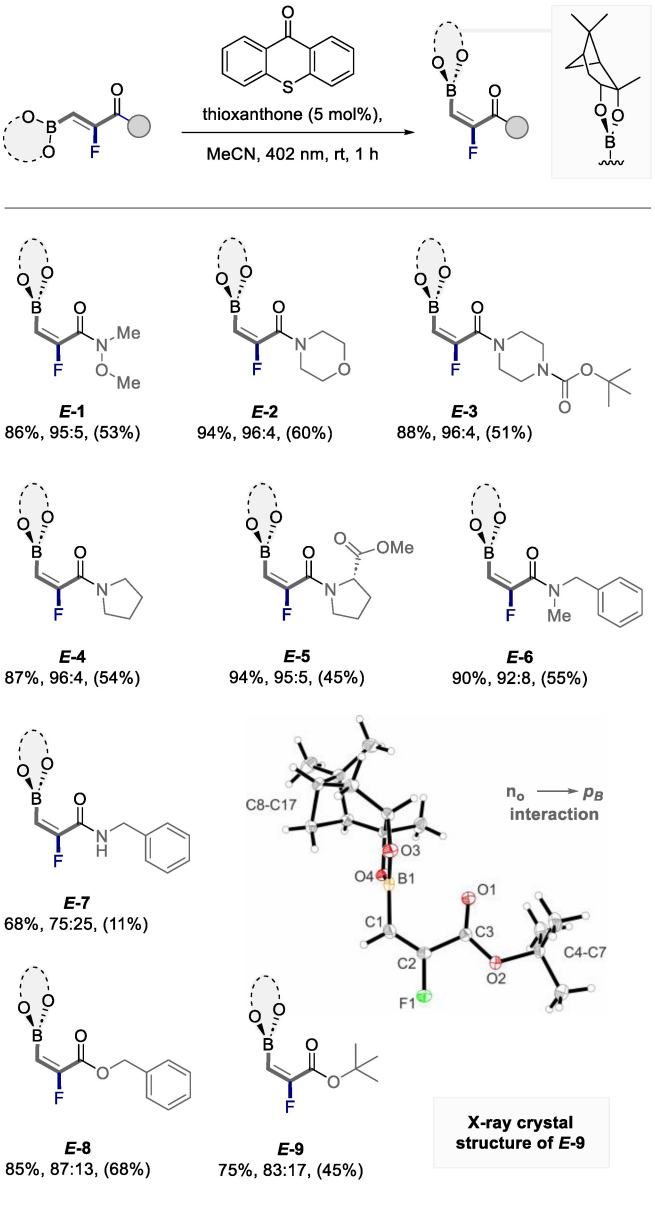

Figure 3. Scope and limitations of the energy transfer-enabled isomerisation and X-ray crystal structure analysis illustrating the origin of selectivity. Thermal ellipsoids are shown at 50% probability. Isolated yields given in parenthesis. $E:Z$ ratios determined by ^{1}H NMR spectroscopy of the crude reaction mixture. Isolated yield of major isomer.

Replacing the Weinreb amide (***E*-1**, *E*/*Z* 95:5) by cyclic secondary amides was found to have little effect on the reaction outcome. This enabled morpholine ***E*-2** and piperidine ***E*-3** to be prepared with high levels of *E*-selectivity (*E*/*Z* 96:4). The ring size also proved to be inconsequential, with the pyrolidine (***E*-4**) and proline (***E*-5**) derivatives being generated with *E*/*Z* selectivities of 96:4 and 95:5, respectively.

Acyclic amides were also found to be compatible with the reaction conditions (***E*-6**, *E*:*Z* 92:8) but it is interesting to note that the isomerisation of secondary amides, such as ***E*-7**, occurred with a reduction in selectivity (*E*:*Z* 75:25). Extension of the scope to esters was also possible as is illustrated by the benzyl and *tert*-butyl derivatives ***E*-8** and ***E*-9**, respectively.

Gratifyingly it was possible to isolate a crystal of ***E*-9** that was suitable for X-ray crystallographic analysis.[28] This revealed a 90° rotation of the C(sp^2)–B bond to allow for a stabilising interaction between the oxygen of the carbonyl group and the empty *p*-orbital of the boron substituent (please see Figure 4, bottom and the Supporting Information).

Bifurcation of the chromophore raises the triplet energy, thereby providing a structural foundation to rationalise selective energy transfer. This triplet energy change was confirmed by kinetic measurements and DFT calculations (see mechanistic studies for Weinreb amide **1** presented below). It is pertinent to note that the B–O distance between the boron and the carbonyl oxygen in compounds ***E*-9** and ***Z*-14** is almost identical (B1–O1: 2.646 Å for ***E*-9** and B1–O3: 2.657 Å for ***Z*-14**, respectively), and the boron coordination geometry remains trigonal planar.

To investigate the impact of the halogen substituent on the efficiency of the energy transfer process, a comparative analysis of the H, F, Cl series based on compound ***E*-8** was conducted (Figure 3, bottom). Under the standard reaction conditions, the photostationary state composition of the non-halogenated species was highest (*Z*:*E* = 93:7), and systematic decreases in selectivity were observed in the order H > F > Cl. This experimental observation is in line with the impact of *para*-substituents on the triplet energies of *trans*-stilbenes, which follow the order H ≥ F > Cl > Br > I.[29]

To further expand the method to tetrasubstituted alkenes, a series of β-Me derivatives were exposed to the standard isomerisation conditions (Figure 4). Gratifyingly, it was possible to isolate ***Z*-10** in 70 % yield with high levels of stereoselectivity (*Z*:*E* 93:7). Moreover, replacing the Weinreb amide by an ester functionality did not impede the reaction, and allowed ***Z*-11** to be generated with a *Z*/*E*-ratio of 98:2. The reaction conditions were also found to be compatible with pinacol boronic esters such as the Weinreb amide ***Z*-12** and tertiary amide ***Z*-13** (up to *Z*:*E* = 94:6).

Crystal structure analysis of the substrate and product isomers ***E*-14**[28] and ***Z*-14**[28] provided an additional insight to support the proposed origin of selectivity. In the starting *E*-isomer, the chromophore is fully conjugated with the boron *p*-orbital aligned with the enone π-system. Upon isomerisation, the C(sp^2)–B bond is no longer in conjugation but

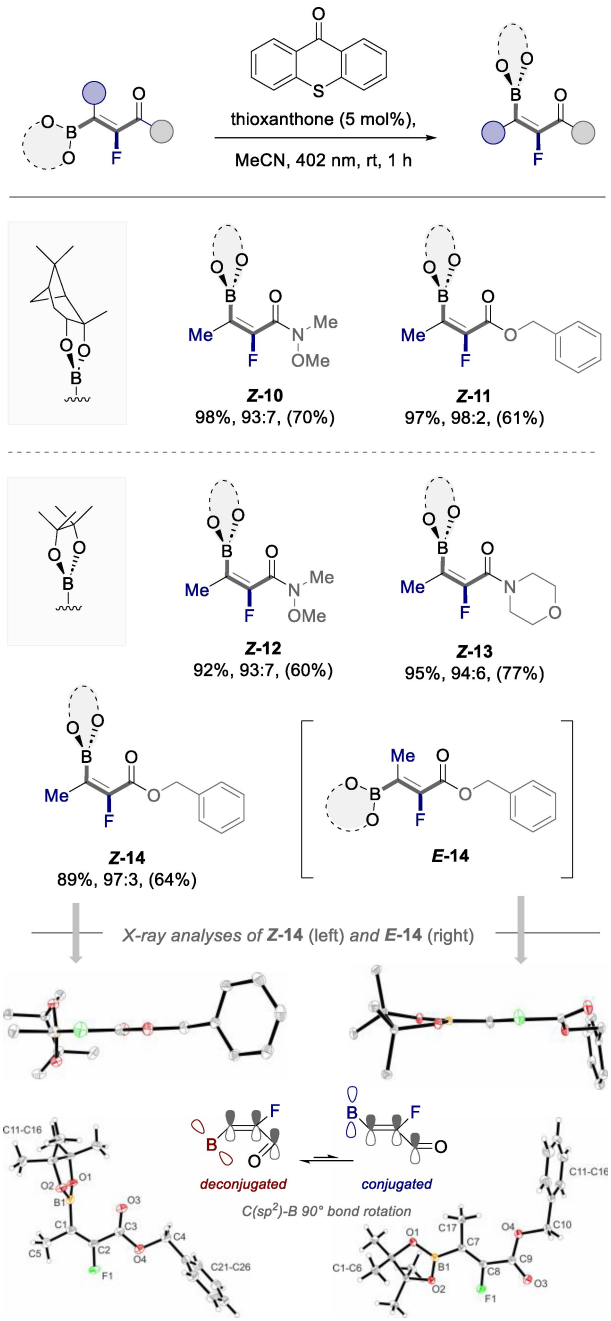

Figure 4. Scope and limitations of the energy transfer-catalysed isomerisation of tetra-substituted alkenes and crystal structure analysis to rationalise the origin of selectivity. Thermal ellipsoids are shown at 50% probability. Isolated yields given in parenthesis. *E*:*Z* ratios determined by ^{1}H NMR spectroscopy of the crude reaction mixture. Please note that the IUPAC descriptors (*E* and *Z*) are inverted relative to Figure 3 on account of the higher priority of the methyl group versus B (In Figure 4, C > B; In Figure 3 B > H).

lies orthogonal to the π-orbitals. The bifurcation of the chromophore is compensated by a stabilising $n_O \rightarrow p_B$ interaction, which prevents re-excitation and allows the two alkene isomers to be photochemically distinguished.

To demonstrate the synthetic utility of the isomerisation in synthesis, the stereocontrolled construction of retinoid-

like fluorinated polyenes was conducted (Scheme 1).[30] To that end, aryl bromide **15** was prepared in two steps from commercial 2-bromophenol, and subjected to a stereospecific cross-coupling with ***Z*-10** to yield Weinreb amide **16** in 74 % yield. The configuration of the fluoroalkene was unequivocally established by single crystal X-ray diffraction.[28] This simple sequence illustrates the value of the C(sp^2)-substituent as a traceless chromophore extension. Following the successful installation of the first fluorinated alkene unit in a *Z*-selective fashion, subsequent reduction of the Weinreb amide was conducted to generate aldehyde **17**. Utilising the elegant boron-Wittig reaction developed by Morken and co-workers,[31] boronic ester **18** was synthesised in 68 % yield. Subsequent bromodeboronation provided access to the intermediate vinyl bromide **19** in preparation for subsequent coupling events. From this common precursor, a second stereospecific coupling reaction with ***E*-20** was performed to generate triene **21**, which is an analogue of the potential type 2 diabetes treatment CS018.[32] To further illustrate the modularity of this approach to fluorinated polyenes, bromine **19** was unified with ***E*-9** to yield the difluorinated triene **22** in 78 % yield.

Finally, the photoisomerisation was investigated by laser flash photolysis (LFP, see Supporting Information for details). Mechanistic studies with thioxanthone (TX) as the catalyst cannot be performed via straightforward emission quenching experiments owing to the non-emissive nature of its photoactive triplet state. Therefore, the sensitised isomerisation by TX of ***E*-1** and ***Z*-1** was studied by LFP with 355 nm laser pulses (Figure 5A) ensuring selective TX excitation. The triplet state of TX is characterised by two main absorption peaks at 315 nm and 625 nm that are

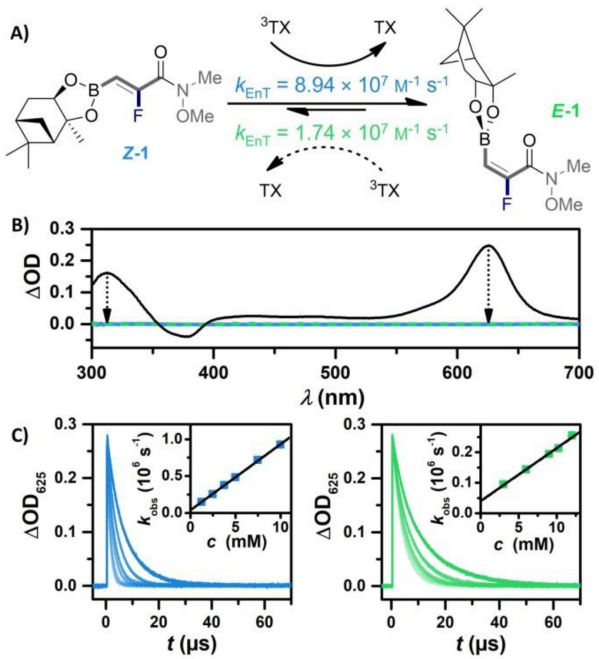

Figure 5. Sensitised isomerisation of ***E*-1** and ***Z*-1** studied by LFP with 355 nm laser pulses in deaerated MeCN. A) Structures and triplet-triplet energy transfer rates using TX as sensitiser. B) TA spectra of 50 μM TX (black, recorded 1 μs after excitation) in the absence of quencher and with 10 mM ***E*-1** (green, recorded 40 μs after excitation) or ***Z*-1** (blue, recorded 11 μs after excitation). C) Quenching experiments of ^{3}TX with varying concentrations of ***Z*-1** (left) and ***E*-1** (right). Inset: Corresponding Stern–Volmer analysis.

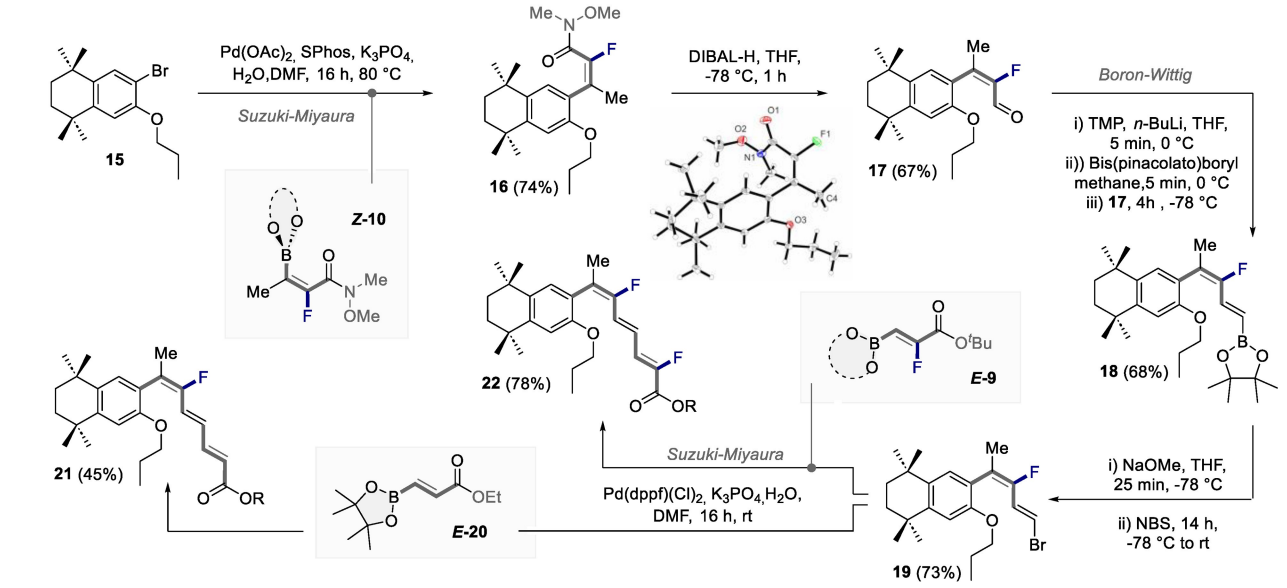

Scheme 1. Application of the photocatalytic isomerisation of alkenyl fluorides in the stereocontrolled syntheses of fluorinated retinoids **21** and **22**. Crystal structure of compound **16**. Thermal ellipsoids are shown at 50 % probability.

observable in the transient absorption (TA) spectrum with a natural lifetime of ≈73 μs (Figure 5B) under these conditions. In the presence of either isomer, the triplet state is quenched and only baseline level is observed following ^{3}TX deactivation. Electron transfer (ET) or hydrogen atom transfer (HAT) reactions with the participation of TX or similar derivatives would unavoidably result in pronounced TX-derived signals in the TA spectra,[33] which is not the case. Taking the quenching efficiencies exceeding 70 %, and the high sensitivity of the employed apparatus into account, the baseline-like spectra are in excellent agreement with triplet-triplet energy transfer (EnT) as being the only reaction pathway in the isomerisation reaction of ***E*-1** and ***Z*-1**:[34] the very short lifetime of the acceptor triplet obtained is also typical behavior of triplet-excited olefins. Stern–Volmer experiments were then conducted with varying concentrations of both isomers, and revealed a faster EnT rate for ***Z*-1** (8.94×10^7 M^{-1}s^{-1}) than for ***E*-1** (1.74×10^7 M^{-1}s^{-1}) by as much as a factor of five. These results indicate an increased triplet state energy of ***E*-1**, which is in line with the chromophore shortening to enable the $n_o\rightarrow p_B$ interaction. Moreover, ***Z*-1** is converted to the perpendicular triplet more rapidly than the corresponding *E* isomer (Figure 1), which results in a photostationary state enriched with ***E*-1**. These spectroscopic findings are not only in line with the experimentally observed composition of the photocatalytic mixture after lab-scale photoirradiation, but they also follow the triplet energy trend calculated using DFT methods (see Supporting Information).

Conclusion

In conclusion, an operationally simple geometric isomerisation of alkenyl fluorides has been enabled by selective energy transfer catalysis using inexpensive thioxanthone (up to *E*/*Z* 98:2 in 1 h). Aided by X-ray structural analysis, the selectivity of the process can be rationalised by chromophore bifurcation in the product: this is a consequence of a stabilising $n_o\rightarrow p_B$ interaction that requires 90° rotation of the C(sp^2)–B bond. This enabling process eliminates the current reliance on lengthy, independent synthesis campaigns to compare the biological effects of monofluoro alkene geometry in amide and polyene biomimetics. The transformation has been validated in bidirectional synthesis campaigns using an ambiphilic linchpin, and showcased in the stereocontrolled syntheses of fluorinated retinoid analogues. It is envisaged that this platform will contribute to the growing arsenal of enabling technologies to facilitate catalyst-based stereodivergent synthesis.[35]

Acknowledgements

We acknowledge generous financial support from the WWU Münster, the JGU Mainz, the Alexander von Humboldt Foundation (fellowship to C.M.), the German Federal Environmental Foundation (DBU, grant number 20022/028) and the European Union Horizon 2020 research and innovation programme under the Marie Skłodowska-Curie grant agreement No 956324 (PhotoReAct) (fellowship to B.K.). Open Access funding enabled and organized by Projekt DEAL.

Conflict of Interest

The authors declare no conflict of interest.

Data Availability Statement

The data that support the findings of this study are available in the Supporting Information of this article.

Keywords: Bioisosteres · Catalysis · Fluorine · Isomerisation · Polyenes

[1] S. Kumari, A. V. Carmona, A. K. Tiwari, P. C. Trippier, *J. Med. Chem.* **2020**, *63*, 12290–12358.
[2] S. Lepri, M. Ceccarelli, N. Milani, G. Cruciani, *Proc. Natl. Acad. Sci. USA* **2017**, *114*, E3178–E3187.
[3] a) R. J. Abraham, S. L. R. Ellison, P. Schonholzer, W. A. Thomas, *Tetrahedron* **1986**, *42*, 2101–2110; b) G. Fischer, *Chem. Soc. Rev.* **2000**, *29*, 119–127.
[4] For studies describing the influence of amide orientation on biological activity see: a) A. Niida, K. Tomita, M. Mizumoto, H. Tanigaki, T. Terada, S. Oishi, A. Otaka, K. I. Inui, N. Fujii, *Org. Lett.* **2006**, *8*, 613–616; b) X. J. Wang, B. Xu, A. B. Mullins, F. K. Neiler, F. A. Etzkorn, *J. Am. Chem. Soc.* **2004**, *126*, 15533–15542; c) M. Marraud, V. Dupont, V. Grand, S. Zerkout, A. Lecoq, G. Boussard, J. Vidal, A. Collet, A. Aubry, *Biopolymers* **1993**, *33*, 1135–1148.
[5] a) T. Allemendinger, E. Felder, E. Hungerbuehler in *ACS Symposium Series 456* (Ed.: J. T. Welch), American Chemical Society, Washington, **1991**, pp. 186–195; b) P. A. Bartlett, A. Otake, *J. Org. Chem.* **1995**, *60*, 3107–3111; c) "Fluorinated Moieties for Replacement of Amide and Peptide Bonds": T. Taguchi, H. Yanai in *Fluorine in Medicinal Chemistry and Chemical Biology* (Ed.: I. Ojima), Wiley, Hoboken, **2009**; d) S. Couve-Bonnaire, D. Cahard, X. Pannecoucke, *Org. Biol. Chem.* **2007**, *5*, 1151–1157; e) N. A. Meanwell, *J. Med. Chem.* **2011**, *54*, 2529–2591; f) G. Landelle, M. Bergeron, M.-O. Turcotte-Savard, J.-F. Paquin, *Chem. Soc. Rev.* **2011**, *40*, 2867–2908; g) M. Drouin, J.-D. Hamel, J.-F. Paquin, *Synthesis* **2018**, *50*, 881–995.
[6] a) D. O'Hagan, *Chem. Soc. Rev.* **2008**, *37*, 308–319; b) L. E. Zimmer, C. Sparr, R. Gilmour, *Angew. Chem.* **2011**, *123*, 12062.
[7] S. Osada, S. Sano, M. Ueyama, Y. Chuman, H. Kodama, K. Sakaguchi, *Bioorg. Med. Chem.* **2010**, *18*, 605–611.
[8] R. A. Altman, K. K. Sharma, L. G. Rajewski, P. C. Toren, M. J. Baltezor, M. Pal, S. N. Karad, *ACS Chem. Neurosci.* **2018**, *9*, 1735–1742.
[9] a) R. Jogireddy, S. Barluenga, N. Winssinger, *ChemMedChem* **2010**, *5*, 670–673; b) H. Du, T. Matsushima, M. Spyvee, M. Goto, H. Shirota, F. Gusovsky, K. Chiba, M. Kotake, N. Yoneda, Y. Eguchi, L. DiPietro, J.-C. Harmange, S. Gilbert, X.-Y. Li, H. Davis, Y. Jiang, Z. Zhang, R. Pelletier, N. Wong, H. Sakurai, H. Yang, H. Ito-Igarashi, A. Kimura, Y. Kuboi, Y. Mizui, I. Tanaka, M. Ikemori-Kawada, Y. Kawakami, A.

Inoue, T. Kawai, Y. Kishi, Y. Wang, *Bioorg. Med. Chem. Lett.* **2009**, *19*, 6196–6199.
[10] Y. Song, L. Clizbe, C. Bhakta, W. Teng, W. Li, P. Wong, B. Huang, U. Sinha, G. Park, A. Reed, R. M. Scarborough, B. Y. Zhu, *Bioorg. Med. Chem. Lett.* **2002**, *12*, 2043–2046.
[11] a) M. Kajjout, M. Smietana, J. Leroy, C. Rolando, *Tetrahedron Lett.* **2013**, *54*, 1658–1660; b) G. Hirai, E. Nishizawa, D. Kakumoto, M. Morita, M. Okada, D. Hashizume, S. Nagashima, M. Sodeoka, *Chem. Lett.* **2015**, *44*, 1389–1391.
[12] a) A. K. Ghosh, B. Zajc, *Org. Lett.* **2006**, *8*, 1553–1556; b) B. Zajc, S. Kake, *Org. Lett.* **2006**, *8*, 4457–4460; c) E. Pfund, C. Lebargy, J. Rouden, T. Lequeux, *J. Org. Chem.* **2007**, *72*, 7871–787; d) A. K. Ghosh, S. Banerjee, S. Sinha, S. B. Kang, B. Zajc, *J. Org. Chem.* **2009**, *74*, 3689–3697; e) M. He, A. K. Ghosh, B. Zajc, *Synlett* **2008**, 999–1004; f) C. Calata, E. Pfund, T. Lequeux, *Tetrahedron Lett.* **2011**, *67*, 1398–1405.
[13] a) J. T. Welch, R. W. Herbert, *J. Org. Chem.* **1990**, *55*, 4782–4784; b) L. G. Boros, B. De Corte, R. H. Gimi, J. T. Welch, Y. Wu, R. E. Handschumacher, *Tetrahedron Lett.* **1994**, *35*, 6033–6036.
[14] M.-H. Yang, S. S. Matikonda, R. A. Altman, *Org. Lett.* **2013**, *15*, 3894–3897.
[15] For selected reviews, see: a) H. Yanai, T. Taguchi, *Eur. J. Org. Chem.* **2011**, 5939–5954; b) M. Drouin, J.-D. Hamel, J.-F. Paquin, *Synthesis* **2018**, *50*, 881–955.
[16] For selected examples, see a) H. Machleidt, R. Wessendorf, *Justus Liebigs Ann. Chem.* **1964**, *674*, 1–10; b) G. E. Moghadam, J. Seyden-Penne, *Bull. Soc. Chim. Fr.* **1985**, 448–454; c) Y. Yamaki, A. Shigenaga, J. Li, Y. Shimohigashi, A. Otaka, *J. Org. Chem.* **2009**, *74*, 3278–3285.
[17] S. Fustero, A. Simón-Fuentes, P. Barrio, G. Haufe, *Chem. Rev.* **2015**, *115*, 871–930.
[18] A. Nouaille, X. Pannecoucke, T. Poisson, S. Couve-Bonnaire, *Adv. Synth. Catal.* **2021**, *363*, 2140–2147.
[19] Q. Liu, Y. Mu, T. Koengeter, R. R. Schrock, A. H. Hoveyda, *Nat. Chem.* **2022**, *14*, 463–473.
[20] H. Sakaguchi, Y. Uetake, M. Ohashi, T. Niwa, S. Ogoshi, T. Hosoya, *J. Am. Chem. Soc.* **2017**, *139*, 12855–12862.
[21] G. Dutheuil, C. Paturel, X. Lei, S. Couve-Bonnaire, X. Pannecouke, *J. Org. Chem.* **2006**, *71*, 4316–4319.
[22] For reviews on photocatalytic geometric alkene isomerisation, see a) T. Neveselý, M. Wienhold, J. J. Molloy, R. Gilmour, *Chem. Rev.* **2022**, *122*, 2650–2694; b) A. Marotta, C. E. Adams, J. J. Molloy, *Angew. Chem. Int. Ed.* **2022**, *61*, e202207067; c) J. J. Molloy, T. Morack, R. Gilmour, *Angew. Chem. Int. Ed.* **2019**, *58*, 13654–13664; d) J. B. Metternich, R. Gilmour, *Synlett* **2016**, *27*, 2541–2552.
[23] a) J. J. Molloy, M. Schäfer, M. Wienhold, T. Morack, C. G. Daniliuc, R. Gilmour, *Science* **2020**, *369*, 302–306; b) M. Wienhold, J. J. Molloy, C. G. Daniliuc, R. Gilmour, *Angew. Chem. Int. Ed.* **2021**, *60*, 685–689.
[24] For an application in dual activation tandem catalysis, see: J. Corpas, M. Gomez-Mendoza, J. Ramírez-Cárdenas, V. A. de la Peña O'Shea, P. Mauleón, R. Gómez Arrayás, J. C. Carretero, *J. Am. Chem. Soc.* **2022**, *144*, 13006–13017.
[25] A. A. Berger, J.-S. Völler, N. Budisa, B. Koksch, *Acc. Chem. Res.* **2017**, *50*, 2093–2103.
[26] T. Neveselý, J. J. Molloy, C. McLaughlin, L. Brüss, C. G. Daniliuc, R. Gilmour, *Angew. Chem. Int. Ed.* **2022**, *61*, e202113600.
[27] a) D. G. Hall, *Structure, Properties, and Preparation Of Boronic Acid Derivatives. Overview of Their Reactions and Applications*, Wiley-VCH, Weinheim, **2005**; b) T. Kinzel, Y. Zhang, S. L. Buchwald, *J. Am. Chem. Soc.* **2010**, *132*, 14073–14075; c) P. A. Cox, M. Reid, A. G. Leach, A. D. Campbell, E. J. King, G. C. Lloyd-Jones, *J. Am. Chem. Soc.* **2017**, *139*, 13156–13165.
[28] Deposition Numbers 2249213 (for ***E*-9**), 2249215 (for ***E*-14**), 2249214 (for ***Z*-14**), and 2250334 (for ***Z*-16**) contains the supplementary crystallographic data for this paper. These data are provided free of charge by the joint Cambridge Crystallographic Data Centre and Fachinformationszentrum Karlsruhe Access Structures service.
[29] H. Görner, *J. Phys. Chem.* **1989**, *93*, 1826–1832.
[30] B. H. Lipshutz, G. C. Clososki, W. Chrisman, D. W. Chung, D. B. Ball, J. Howell, *Org. Lett.* **2005**, *7*, 4561–4564.
[31] J. R. Coombs, L. Zhang, J. P. Morken, *Org. Lett.* **2015**, *17*, 1708–1711.
[32] a) T. Deng, S. Shan, Z. Bin Li, Z. W. Wu, C. Z. Liao, B. Ko, X. P. Lu, J. Cheng, Z. Q. Ning, *Biol. Pharm. Bull.* **2005**, *28*, 1192–1196; b) S. S. Canan Koch, L. J. Dardashti, J. J. Hebert, S. K. White, G. E. Croston, K. S. Flatten, R. A. Heyman, A. M. Nadzan, *J. Med. Chem.* **1996**, *39*, 3229–3234.
[33] a) S. F. Yates, G. B. Schuster, *J. Org. Chem.* **1984**, *49*, 3349–3356; b) M. R. Rodrigues, M. G. Neumann, *Macromol. Chem. Phys.* **2001**, *202*, 2776–2782.
[34] a) A. Luque, J. Groß, T. J. B. Zähringer, C. Kerzig, T. Opatz, *Chem. Eur. J.* **2022**, *28*, e20210432; b) Y. Liu, D. Ni, B. G. Stevenson, V. Tripathy, S. E. Braley, K. Raghavachari, J. R. Swierk, M. K. Brown, *Angew. Chem. Int. Ed.* **2022**, *61*, e202200725.
[35] S. Krautwald, E. M. Carreira, *J. Am. Chem. Soc.* **2017**, *139*, 5627–5639.

Manuscript received: March 22, 2023
Accepted manuscript online: May 5, 2023
Version of record online: May 24, 2023